Biomass Conversion and Biorefinery (2023) 13:10133–10146
https://doi.org/10.1007/s13399-021-01873-4

ORIGINAL ARTICLE

Green biosynthesis of zinc and selenium oxide nanoparticles using callus extract of *Ziziphus spina-christi*: characterization, antimicrobial, and antioxidant activity

Islam Iashin[1] · Mohamed Hasanin[2] · Sayed A. M. Hassan[3] · Amr Hosny Hashem[1]

Received: 1 June 2021 / Revised: 1 August 2021 / Accepted: 12 August 2021 / Published online: 24 August 2021

Abstract
In this present work, the plant tissue culture biotechnology was used as good approach for green biosynthesis of nanoparticles (NPs) because it is safe, clean method, and ecofriendly. Zinc and selenium oxide nanoparticles were biosynthesized using callus extract of *Ziziphus spina-christi* for the first time. Callus culture from young leaf of *Ziziphus spina-christi* on medium supplemented with 1 mg/L 2,4-dichlorophenoxy acetic acid (2,4-D) produced the highest significant callus fresh weight (12 g), color, and development. The characterization of ZnONPs and SeONPs was carried out using UV–vis, FTIR, XRD, SEM, TEM, and thermal analysis; results revealed that prepared ZnONPs and SeONPs are crystalline in nanoscale with particle size between 20 and 45 nm. Antimicrobial activity of ZnONPs and SeONPs was evaluated, and results illustrated that both ZnONPs and SeONPs have potential antimicrobial activity against common human pathogens such as Gram-negative bacteria, Gram-positive bacteria, and unicellular and multicellular fungi, where SeO-NPs had antimicrobial activity higher than ZnONPs. Moreover, ZnONPs and SeONPs have a promising antioxidant activity as well as low toxicity on 1- BJ1 normal cells. Finally, a promising green biosynthesized ZnONPs and SeONPs have potential antimicrobial activity as well as antioxidant activity which will be applied for controlling of resistant microorganism.

Keywords Zinc nanoparticles · Selenium nanoparticles · Callus · Antimicrobial activity · *Ziziphus spina-christi* · Antioxidant activity

1 Introduction

Antimicrobial resistance and food safety have become two of the major health apprehensions for the public, government, and regulatory agencies in the last two decades [1]. The infectious diseases are the primary causes of deaths that occur worldwide. Antibiotics resistance is considered one of one of the most problems which affect human life. Likewise, antifungal resistance causes great threat on human health. Invasive fungal infections for human are candidiasis and aspergillosis [2, 3]. Therefore, there is a necessity to synthesize or design alternative compounds which have potential antimicrobial and antioxidant activity through green and ecofriendly method.

Nanotechnology is an emerging field in science, which deals with the biology, chemistry, physics, and engineering. The term "nano" refers to the size of the particle that ranges from 1 to 100 nm [4]. Nanobiotechnology is a branch from nanotechnology, and it is the application of nanotechnology in biological fields [5, 6]. Metal nanoparticles are widely used as antimicrobial and antioxidant as Ag-NPs, Zn-NPs, SeNPs, and Cu-NPs [7–13]. There are several methods for nanoparticle synthesis as physical, chemical, and biological methods, but the biological methods involving the plants or microorganism for the synthesis

✉ Mohamed Hasanin
sido_sci@yhoo.com

✉ Amr Hosny Hashem
amr.hosny86@azhar.edu.eg

[1] Botany and Microbiology Department, Faculty of Science, Al-Azhar University, Cairo 11884, Egypt

[2] Cellulose & Paper Department, National Research Centre, 33 El Bohouth St., Dokki, P.O. 12622, Giza, Egypt

[3] Tissue Culture Technique Lab, Central Laboratories Network and Pomology Department, National Research Centre, 33 El Bohouth St., Dokki, P.O. 12622, Giza, Egypt

are more preferred due to the chemical and physical methods need high thermal conditions, hazardous chemicals, and acidic pH which is extremely toxic and unsafe for biological applications [14, 15]. Green chemistry approach emphasizes the use of natural organisms, microorganism, microalgae, enzyme, plant, and plant extracts, and offers a reliable, simple, nontoxic, low-cost approach, stable nature, and eco-friendly [16, 17]. Plants have been used for metal nanoparticle biosynthesis such as selenium [18], ZnO [19], Au_2O_3 [20], MgO [21], CuO [22], SnO_2 [23], NiO [24], and silver nanoparticles [25]. Zinc oxide nanoparticles were synthesized previously using different plant extracts as *Lippia adoensis* [26], *Sambucus ebulus* [27], *Hibiscus subdariffa* [28], *Matricaria chamomilla* & *Lycopersicon esculentum* [29], *Cassia fistula & Melia azadarach* [19], and *Aloe vera* [30]. Likewise, selenium nanoparticles were synthesized using *Aloe vera* [31], *Cassia auriculata* [32], *Zingiber officinale* (Ginger) [14], *Withania somnifera* [33], and *Emblica officinalis* [18]. Although, Zn-NPs and Se-NPs are wildly biosynthesized using different plant extract, but did not synthesize previously by *Ziziphus spina-christi*. *Ziziphus spina-christi* (Family: Rhamnaceae) was called sidr (related to the Quranlote trees). It is an important cultivated tree and one of the few truly native tree species of Arabia that is still growing along with many newly introduced exotic plants [34]. The genus *Ziziphus* is known for its medicinal properties as a hypoglycemic, hypotensive, antiinflammatory, antimicrobial, antioxidant, antitumor, and liver protective agent and as an immune system stimulant [35]. Furthermore, *Z. spina-christi* extract has also been reported to possess protective effect against aflatoxicosis [36]. Therefore, this study aimed to biosynthesize of ZnONPs and SeONPs using callus extract of *Ziziphus spina-christi* for the first time. Moreover, to characterize and evaluate ZnONPs and SeONPs as antimicrobial as well as antioxidant activity.

2 Material and methods

2.1 Plant material collection and sterilization of explants

This part was carried out at the Tissue Culture Technique Lab, Central Laboratories Network, National Research Centre, Dokki, Giza, Egypt. Fresh leaves were collected from research and production station of National Research Centre NRC, Al Emam Malek village, Al Nubarie district, Al Behaira Governorate, Egypt. Leaves maintained at room temperature were excised and used as explants. The explants were washed with running tap water for 30 min and surface sterilized with 0.1% (w/v) $HgCl_2$ solution for 10 min and finally the explants were rinsed with sterile distilled water 3 times for 15 min, then sterilized with 10% Clorox (commercial bleach) with 0.1% tween-20 for 15 min then, washed with sterilized distilled water 3 times for 15 min each.

2.2 Callus induction and culture conditions

The prepared explants young leaves were cut in portions of about (1×1 cm) were cultured on MS medium [37] supplemented with different concentration of 2,4-dichlorophenoxy acetic acid (2,4-D) at the rate of 0.5, 1, 2, and 4 mg/L, 30 g/L sucrose, and 7 g/L Difico-Bacto agar which was considered as basal medium. The pH of the medium was adjusted at 5.8 and autoclaved at 121 °C and 1.5 Ib/inch^2 for 25 min. All the cultures were incubated in the culture room under controlled conditions, where temperature was maintained at 25 ± 2 °C and kept under dark conditions in order to callus induction, the cultures were incubated at 26 ± 1 °C in the dark conditions. Callus parameters were recorded after four subculture each one (4 weeks).

2.3 Preparation of aqueous callus extract and biosynthesis of ZnONPs and SeONPs

Simply, the oven dry callus was ground and suspended in Millipore water with concentrations 1, 3, and 5% (wt/v). The mixture was sonicated in sonication water path for 60 min at 40 °C. Cooled extract was filtrated through filter paper No. 1. The filtrate total extract was used for biosynthesis of ZnONPs and SeONPs in concentration 1 mM of each metal. The preparation of ZnONPs and SeONPs was performed using zinc acetate and selenium oxide respectively. The reaction mixture was incubated for 24 h at 37 °C.

2.4 Characterization of ZnONPs and SeONPs

Investigation of the produced nanoparticle structural changes of different samples was performed by UV–visible (UV–vis) spectroscopy of the prepared ZnONPs and SeONPs (colloidal form) which were measured on V-630 UV–vis spectrophotometer (Jasco, Japan) in the range of 1000–200 nm. ATR-FTIR spectroscopy of samples in powder form (Spectrum Two IR Spectrometer – Perk in Elmer, Inc., Shelton, USA), all spectra were obtained by 32 scans and 4 cm^{-1} resolution in wavenumbers ranging from 4000 to 400 cm^{-1}. The crystal structure was determined using XRD (Model diffractometer, Shimadzu 7000, Japan.) where the samples were measured as powder. The surfaces of prepared samples (powder form) were investigated by a field emission SEM coupled with energy dispersive X-ray analysis;

Model Quanta 250 FEG (Field Emission Gun) attached with EDX Unit (Energy Dispersive X-ray Analyses) for EDX with accelerating voltage 30 kV. TEM, Model JEM2010, Japan, was used to investigate particle size and morphology of the synthesized samples (powder form). TGA analysis of tested samples (powder form) was carried out using the TGA Q500 device as powder. T!he dynamic light scattering (DLS) of the prepared samples (colloidal form) was measured, using Nicomp™ 380 ZLS size analyzer, USA. Leaser light scattering was used at 170° in case of particle size detection where zeta potential was measured at 18°.

2.5 Antimicrobial activity

Antibacterial activity of biosynthesized ZnONPs and SeONPs using the callus extract of *Ziziphus spina-christi* was evaluated according to agar well diffusion assay by Muller Hinton agar plates against human pathogenic bacterial strains: Gram-negative bacteria (*Escherichia coli* ATCC25922 and *Pseudomonas aeruginosa* ATCC 27,853), Gram-positive bacteria (*Staphylococcus aureus* ATCC25923 and *Bacillus subtilis* ATCC6051). Likewise, antifungal activity was evaluated against unicellular fungi (*Candida albicans* ATCC90028 and *Cryptococcus neoformans* ATCC 14,116) and multicellular fungi (*Aspergillus niger* RCMB 02,724 and *A. fumigatus* RCMB 02,568) using PDA plates. Diameter of inhibition zone was determined by millimeter (mm). Moreover, minimum inhibitory concentration (MIC) of ZnONPs and SeONPs was determined. ZnONPs and SeONPs, Amoxicillin-clavulanic acid (AMC) as a standard antibiotic and Nystatin as a standard antifungal agent, were prepared in different concentrations ranged from 1000 to 15.62 µg/mL, then assessed separately to detect MIC against selected bacterial and fungal strains [38].

2.6 Antioxidant activity

Antioxidant activity of ZnONPs and SeONPs was carried out using DPPH (2, 2-diphenyl-1-picrylhydrazyl) method. Different concentrations of biosynthesized ZnONPs and SeONPs (7.81, 15.62, 31.25, 62.5, 125, 250, 500, 1000, and 2000 µg/mL) were used to determine the ability to scavenge DPPH radicals [39, 40]. A DPPH radical solution (1 mm) was prepared using 95% ethanol, and 800 µL of DPPH solution was mixed with 200 µL of different concentrations of ZnONPs and SeONPs, profusely shake, and finally kept for 30 min at 25˚C in darkness. After this time, centrifugation was performed at 13,000 rpm for 5 min. Absorbance of each concentration was measured at 517 nm against a blank. Ascorbic acid was used as standard. Antioxidant activity of standard and different concentrations of ZnONPs and SeONPs was determined as DPPH scavenging activity (%) calculated by the following equation:

$$\text{Antioxidant activity}\% = \frac{\text{Abs. of control} - \text{Abs. of sample}}{\text{Abs. of control}} \times 100$$

2.7 Cytotoxicity test

The samples were tested against the normal human epithelial cell line 1- BJ1 (normal Skin fibroblast) in different concentrations (1000, 500, 250, 125, 62.5, 31.25, and zero µg/mL as control of each sample (total extract, ZnONPs, and SeONPs). In vitro bioassay was conducted and determined by the Bioassay-Cell Culture Laboratory, National Research Centre, El-Tahrir St., Dokki, Cairo 12,622, Egypt.

2.8 Statistical analysis

All the experiments were done in triplicate and statistical analysis was carried out using Minitab software (version 18). The values were given as mean ± SD (standard deviations). Levels of significance were considered at $p \leq 0.05$. Statistical analysis was investigated by ANOVA (one-way analysis of variance) Tukey method for the obtained results.

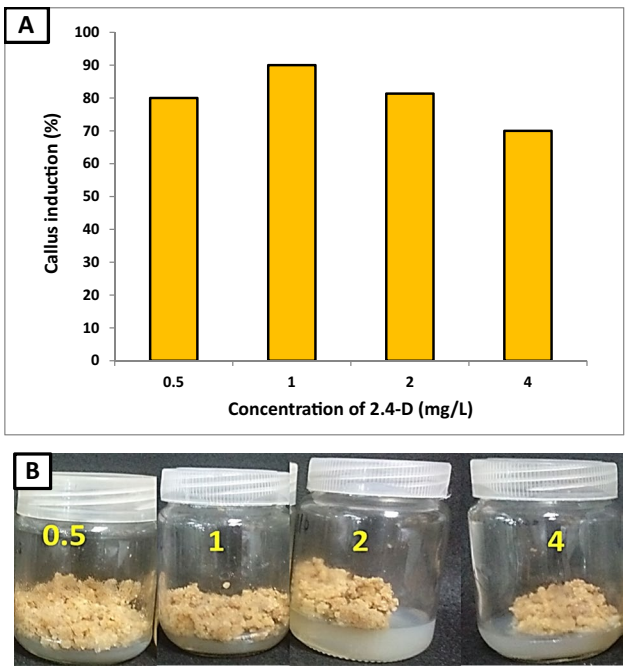

Fig. 1 Effect of different concentrations of 2,4-D on callus induction of *Ziziphus spina-Christi* (**A**); Vigorous callus growth on MS media supplemented with different concentrations of 2,4-D (**B**)

3 Results and discussion

3.1 Callus induction and optimization

Figure 1A shows the effect of growth regulators on callus induction and callus production parameters of *Ziziphus spina-christi*. Effects of various media contained different concentrations of 2,4-D (0.5, 1, 2, and 4 mg/L) for callus induction after 4 weeks are shown in Fig. 1. Results illustrated that, the concentration 1 mg/L of 2,4-D was significant among other concentrations for explant-induced callus, where percentage of callus induction was 90%. In Table 1 and Fig. 1B as compared to other treatments, the result showed that the highest weights of callus (12 g/Jar) were obtained from leaf explants cultured on MS media supplemented with 1 mg/L 2,4-D. Decreasing of callus production efficiency was associated with the increasing of 2,4-D concentration up to 2 mg/L (Table 1). Ahmadi et al. [41] illustrated that culture medium containing 2,4-D and TDZ at concentrations of 0.5 and 1 mg/L has the highest for callus induction and formation. Previous studies reported that 2,4-D is the best auxin for callus induction in monocot and even in dicot [42, 43]. On the other hand, callus production and degree for callus formation decrease by increasing concentration of 2,4-D as shown in Fig. 1B and Table 1. The inhibitory effect of 2,4-D with high concentration on callus induction has been reported [44, 45].

Table 1 Effect of different concentrations of 2,4-D on callus formation parameters of *Ziziphus spina-Christi*

Treatments2,4-D mg/l	Necrosis scores	Callus development scores	Callus weight (g)
0.5	2^{b}	4^{b}	10.6^{b}
1	1^{c}	5^{a}	12^{a}
2	2^{b}	3.7^{b}	10.4^{b}
4	4^{a}	3^{c}	9^{c}
LSD	0.472	0.653	0.842

Data are expressed as means ± standard deviations of triplicate assays. The different alphabetic superscripts are significantly different ($p < 0.05$) based on Tuky multiple range test

3.2 Biosynthesis of ZnONPs and SeONPs

Biomolecules present in plant extracts can be used to reduce metal ions to nanoparticles in a single-step green synthesis process [46]. The reducing agents involved include the various water soluble plant metabolites (e.g., alkaloids, phenolic compounds, terpenoids) and co-enzymes [47]. In this study, callus extract of *Ziziphus spina-Christi* was used for ZnONPs and SeONPs biosynthesis. Results showed that, changing the color to yellow and red after mixing callus extract with zinc acetate and selenium oxide, these indicate the formation of ZnONPs and SeONPs respectively. Previous studies reported appearance of yellow color for

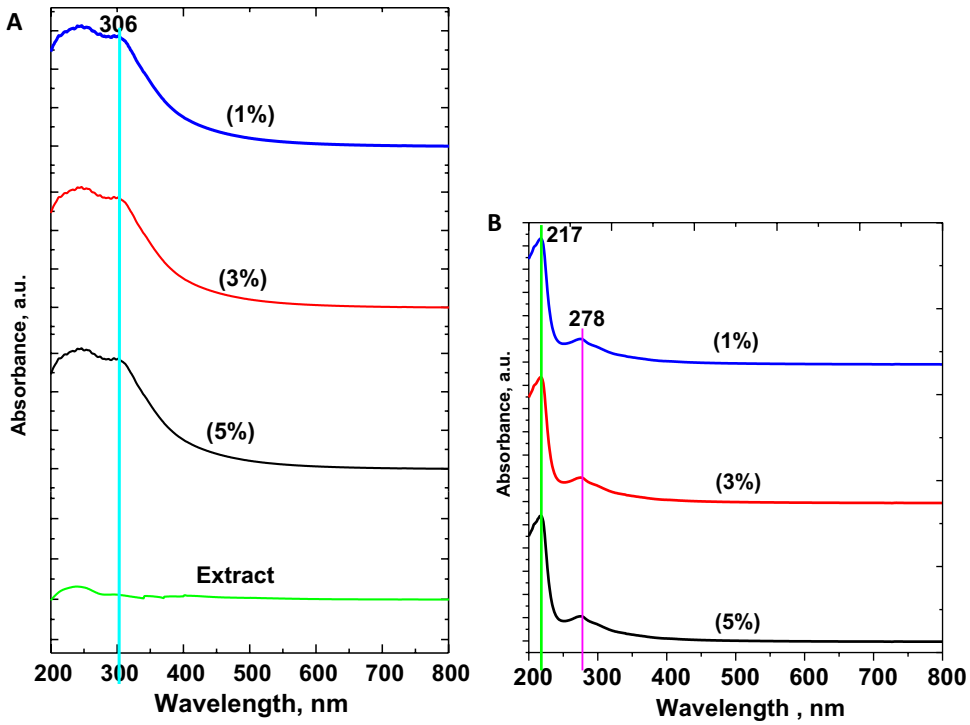

Fig. 2 UV–visible of prepared nanoparticles via different concentrations of total extract (**A**) and ZnONPs as well as SeONPs (**B**)

zinc nanoparticles [19, 48], and red color for selenium nanoparticles [31, 33].

3.3 Characterization of ZnONPs and SeONPs

3.3.1 UV–visible

The UV–visible measurements of the prepared nanoparticles are illustrated in Fig. 2. UV–visible charts of ZnONPs and SeONPs revealed that different concentrations of the extract are not significant effect in the preparation progress. Figure 2A shows the total extract UV–visible spectrum which clarified no band at both UV and visible light. Additionally, ZnONPs UV–visible charts for three concentrations 1, 3, and 5% which seems that the one finger which around 306 nm with a narrow absorption peak which means a good crystalline specimen [49, 50]. On the other hand, the SeONPs charts of concentrations 1, 3, and 5% were observed in Fig. 2B with no difference. In the context, the characteristic peak of preparation SeONPs was observed at 217 and 278 nm [51, 52]. These results confirmed that the preparation of nanoparticles is containing some impurities of the extract component, and by the way, it does not affect the nanoparticle behaviors.

3.3.2 FT-IR

In the present work, the FT-IR is the useful technique to evaluate the function groups in the total extract which act as green tool to reduce the metal size. Figure 3 illustrates the FT-IR spectra of the total extract, ZnONPs, and SeONPs. The total extract spectra assigned characteristic peaks, namely at 3420, 1636, and 1385 cm^{-1} which referred to OH group due to the presence of alcohols, phenols, carbohydrates, etc., amide I (NH) group, and indicating to carboxyl groups, respectively [53, 54]. Additionally, peaks at 1074, 816, and 611 cm^{-1} which assigned to overlapping of amid II of protein and C-H rocking of CH2, aromatic components, and the ring and skeletal modes of the main components have polyhydroxyl structure [55]. On the other hand, the reduction of zinc was affected the total extract FT-IR spectrum where OH band was split into two small peaks at 3262 and 2911 cm^{-1}; this may be due to the interaction of free hydroxyl groups in reducing of Zn to ZnONPs. Moreover, all total extract function groups were shifted to low frequency as well as the fingerprint area was observed a condensed

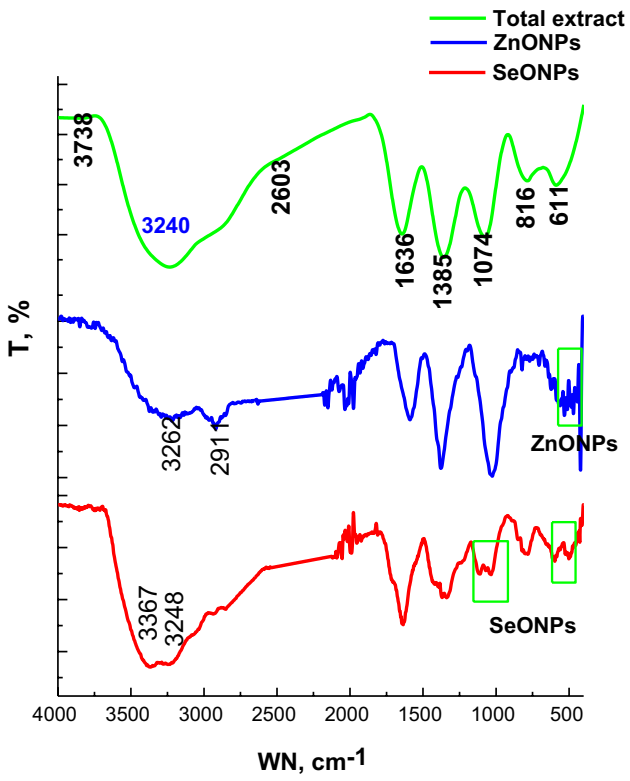

Fig. 3 FT-IR spectra of total extract and prepared ZnONPs and SeONPs

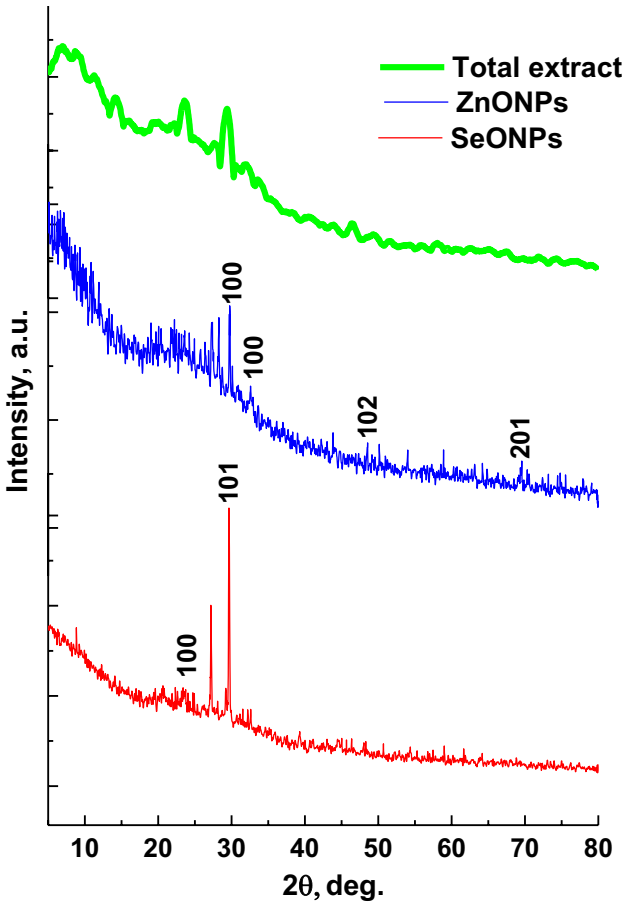

Fig. 4 XRD pattern of total extract and prepared ZnONPs and SeONPs

peak at range 400–500 cm^{-1} which specific to ZnONPs [56]. In case of SeONPs, the main peaks of total extract were changed in intensity and shifted to low frequency as result to reduce the selenium oxide particle size. In addition, many characteristic peaks of selenium were assigned. The peaks at 1128, 1024, and 476 cm^{-1} represent to starching vibration of SeO_2, characteristic Se–O stretching vibration, and bending vibrations of Se–O, respectively [57, 58]

3.3.3 XRD

The XRD patterns of the total extract, ZnONPs, and SeONPs are observed in Fig. 4. The total extract showed a classical organic material XRD pattern with many hubs around 10° as broad bands referred to amorphous structure of organic materials. On the other hand, ZnONPs and SeONPs were observed crystalline behavior according to XRD pattern with overlapping with parent components of total extract. The zinc pattern was appeared as a characteristic peaks at 100, 100, 102, and 201 referred to 29.8, 32.1, 47.9, and 69.4°, respectively planes of ZnO in the wurtzite structure corresponding with JCPDS (Card Number 36–1451) [59]**.** In addition, the XRD patterns of SeONPs shown at 2θ = 38·46° indicates the presence of impurity. It is observed from 1-h pattern that two peaks emerging at 2θ = 23·56° and 29·72° are assigned to (1 0 0) and (1 0 1) planes, respectively, of trigonal selenium (t-Se) (JCPDS card no. 06–0362) [58]. Overall, the XRD patterns observed that the ZnONPs are more crystalline than SeONPs.

3.3.4 Topography

The topography study of prepared ZnONPs and SeONPs was studied via SEM with EDX and TEM with diffraction. SEM images of ZnONPs and SeONPs are observed in Fig. 5A and C ; EDX charts in Fig. 5B and D respectively. The SEM images illustrated that both metal oxide nanoparticles appear as clusters with high aggregations and this may be according to the state of examination where SEM sample was tested as dry. The EDX of both metal oxide nanoparticles showed the presence of carbon, nitrogen, and oxygen with peak of each metal individual. In contrast, the TEM images illustrated

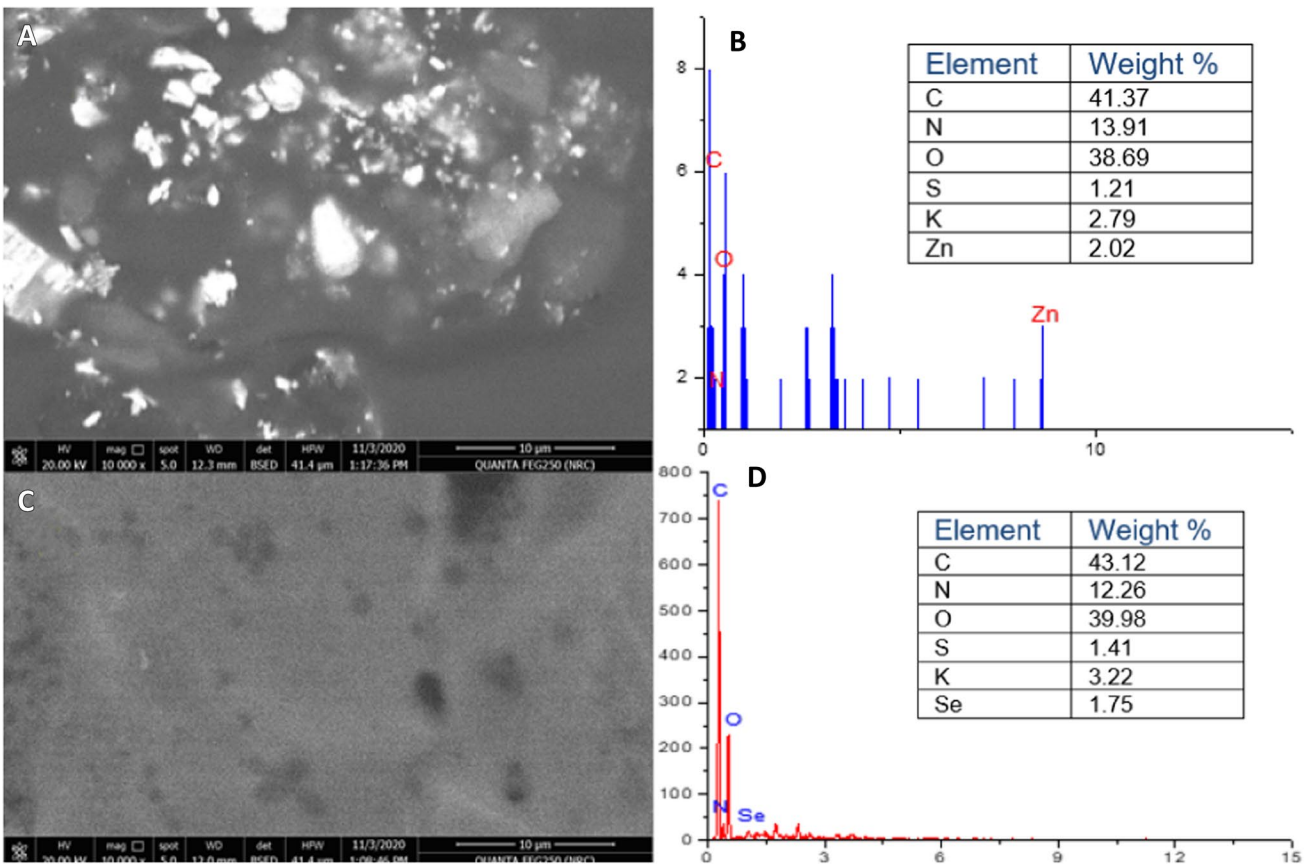

Fig. 5 Topography images of SEM ZnONPs (**A**) and SeONPs (**C**) as well as the EDX chart of ZnONPs (**B**) and SeONPs (**D**)

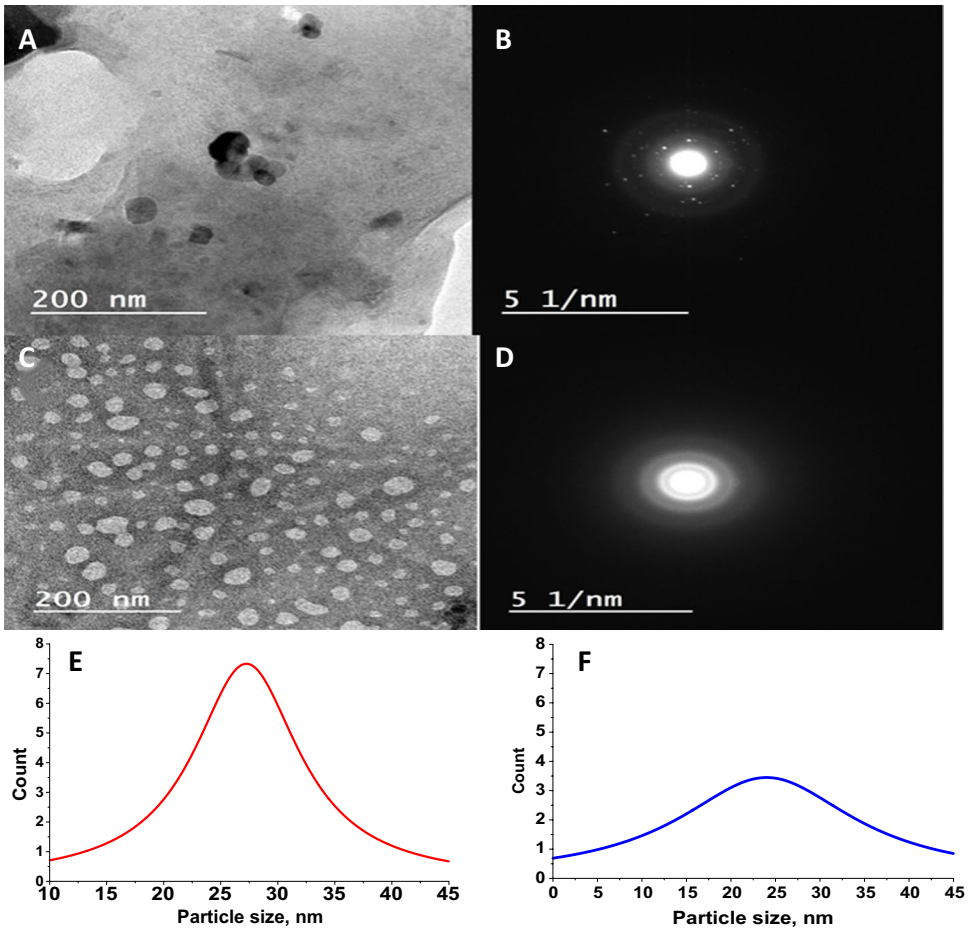

Fig. 6 TEM of ZnONPs (**A**) and SeONPs (**C**) as well as the diffraction of ZnONPs (**B**) and SeONPs (**D**). The size distribution of ZnONPs (**E**) and SeONPs (**F**)

that, prepared metal oxides in nanoscale with diffraction referred to crystallinity. Moreover, the TEM image of ZnONPs (Fig. 6A) and the diffraction (Fig. 6B) revealed that, the particles size is ranged from 20 to 45 nm with high crystallinity. However, the TEM image of SeONPs (Fig. 6C) and the diffraction (Fig. 6D) showed that the particles size is ranged from 15 to 45 nm with low crystallinity as spherical shape. Size distribution is shown in Fig. 6E and H.

3.3.5 Thermal study

The thermal study of the total extract, ZnONPs, and SeONPs was carried out to evaluate the role of plant extract to reduce the metals to nanosize. Figure 7 shows the thermal study included TGA (A) and DTGA (B). The plant extract observed low thermal stability according to the main components is organic compounds with some salts involved in the extract as results to the extraction method. The TGA chart of total extract performed the stable weight loss value after heated to about 600 °C with fixed weight loss around 33%. Additionally, The DTGA curve shows degradation peaks at 305 and 565 °C with weight loss 63 and 38%, respectively. In contrast, the TGA charts of ZnONPs and SeONPs observed the thermal stability up to 1000 °C. Moreover, DTGA chart of ZnONPs shows three main peaks for the thermal degradation at 319, 768, and 940 °C with weight loss 61, 42, and 29%, respectively. In context, SeONPs show the two main peaks for thermal degradation 325 and 905 °C with weight loss 51 and 25%. These results confirm the XRD and topography studies where the crystallinity is playing an important role in thermal stability, whereas, the high crystallinity degree of zinc nanoparticles made their thermal behavior more stable than selenium nanoparticles [9, 60, 61].

3.3.6 DLS

Table 2 observes DLS results, polydispersity index (PDI), and particle size distribution in aqueous solutions with relative concentration. The particle sizes of prepared nanoparticle were recorded as 253 and 287 nm with PDI 0.23 and 0.226 for ZnONPs and SeONPs, respectively. The results of particle size were referred to the many aggressions between

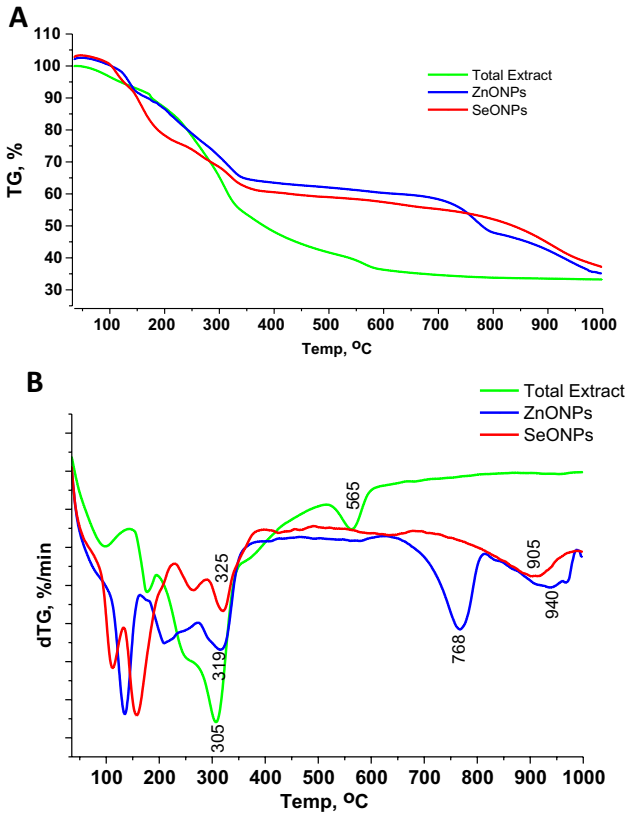

Fig. 7 **A**, **B** Thermal study of total callus extract, ZnONPs, and SeONPs

particles as well as the PDI results were emphasized the homogeneous colloidal solution of nanoparticle. On the other hand, zeta potential zeta measurements are confirmed the aggregations of the particles where the ZnONP and SeONP average zeta values are − 9.60 and 0, respectively in agglomerate window as reported by Kumar, A. and C.K. Dixit [62].

3.3.7 Antimicrobial activity

Due to increasing number of drug resistance by human pathogens, the search of new antimicrobial drugs by green and ecofriendly method is required. Thus, the rapid progression in bionanotechnology spurs significant biosynthesis of new compounds which have good antimicrobial activity. In this study, ZnONPs and SeONPs were biosynthesized using callus extract of *Ziziphus spina-christi*, then were evaluated as antimicrobial agent as shown in Fig. 8. Results illustrated that, both ZnONPs and SeONPs have potential antimicrobial activity against *E. coli*, *P. aeruginosa*, *S. aureus*, *B. subtilis*, *C. albicans*, *C. neoformans*, *A. niger*, and *A. fumigatus.* Figure 8 shows antimicrobial activity of ZnONPs and SeONPs at concentration 1 mM, where inhibitory action of SeONPs more than ZnONPs against all tested microbial strains. Callus extract did not show any inhibition zones against all tested microbial strains except *C. neoformans* where gave inhibition zone 9 mm. On the other hand, ZnONPs gave inhibition zones 15, 11, 13, 27, 19, 37, 17, 16, 26, and 16 mm against *E. coli*, *P. aeruginosa*, *S. aureus*, *B. subtilis*, *C. albicans*, *C. neoformans*, *A. niger*, *A. terreus*, *A. flavus*, and *A. fumigatus* respectively, while as inhibition zones of SeONPs (1 mM) were 31, 35, 25, 35, 45, 56, 29, 25, 22, and 19 mm against *E. coli*, *P. aeruginosa*, *S. aureus*, *B. subtilis*, *C. albicans*, *C. neoformans*, *A. niger*, *A. terreus*, *A. flavus*, and *A. fumigatus* respectively. From this data, the highest inhibitory action of ZnONPs and SeONPs was against *C. neoformans*, while the lowest inhibitory action ZnONPs and SeONPs was against *P. aeruginosa* and *A. fumigatus* respectively.

The lowest concentration of metal nanoparticles that inhibited microbial growth is defined as MIC. Since the inhibitory microbial activities depended on the dose used, it was necessary to determine the lowest dose affecting the pathogenic bacteria [63]. Therefore, MICs of ZnONPs and SeONPs against all tested bacterial and fungal strains were determined as shown in Fig. 9. Results showed that, MICs of SeONPs were better than ZnONPs, where MICs of ZnONPs against all tested strains were in range 0.0312–0.5 mM, while as MICs of SeONPs were in range 0.0078–0.125 mM. MIC of ZnONPs for *C. neoformans* was 0.0312 mM, for *B. subtilis* and *A. flavus* was 0.0625 mM, for *C. albicans* and *A. niger* was 0.125 mM, for *E. coli*, *S. aureus*, *A. terreus*, and *A. fumigatus* was 0.25 mM, and for *P. aeruginosa* was 0.5 mM. On the other hand, MIC of

Table 2 DLS measurements of ZnONPs and SeONPs

	Zeta potential measurements				Particle size	
	Cell current, mA	Av. phase shift, rad/s	Av. mobility, M.U	Av. zeta potential, mV	PDI	Average particle size/nm
ZnONPs	2.34	− 4.13	− 0.67	− 9.60	0.23	253
SeONPs	3.76	0	0	0	0.226	287

SeONPs for *C. neoformans* was 0.0078 mM, for *P. aeruginosa* and *B. subtilis* was 0.0156 mM, for *E. coli*, *C. albicans*, and *A. niger* was 0.0312 mM, for *S. aureus* and *A. terreus* was 0.0625 mM, and for *A. flavus* and *A. fumigatus* was 0.125 mM. Previous studies reported the biosynthesized Zn-NPs and Se-NPs using plant extracts. Gunti et al. [18] used *Emblica officinalis* fruit extract for biosynthesized Se-NPs and reported their antimicrobial activity where MIC was in the range 9.16–59.83 µg/mL. Kokila et al. [64] biosynthesized Se-NPs using leaf extract where it observed antimicrobial activity against *S. aureus*, *E. coli*, and *A. niger*. Moreover, *Withania somnifera* was used in previous study for Se-NP biosynthesis and it exhibited considerable antibacterial activity on *B. subtilis* (12 mm), *Klebsiella pneumoniae* (14 mm), and *S. aureus* (19.66 mm) [33]. The mechanism of ZnONPs and SeONPs is possibly adhering to cell membrane and infiltrate into it causing physical damage, and consequently leakage of cellular constituents with inhibits respiratory enzymes and lead to death of microbial cell [65]. Although, the mechanism of ZnONPs and SeONPs may be the same but the antimicrobial activity of SeONPs was higher than ZnONPs due to difference of particle size in the two metal oxides, the particle size of SeONPs was lower than ZnONPs, where the antimicrobial activity increases with decreasing the particle size [66].

3.3.8 Antioxidant activity

Oxidative damage to biological materials occurs when biological reactions produce reactive oxygen species (ROS) as by-products which cause a cell death [67]. Antioxidant compounds have been used to reduce the harmful effect of ROS. The reducing power of ZnONPs and SeONPs is directly proportional to their antioxidant activity. In the current study, antioxidant activity of biosynthesized ZnONPs and SeONPs was determined using DPPH free radical assay. Scavenging activity of ZnONPs and SeONPs depends on degree of discoloration of purple color of DPPH solution. Figure 10 shows antioxidant activities of ZnONPs and SeONPs at different concentrations 0.0078, 0.0156, 0.0312, 0.0625, 0.125, 0.25, 0.5, and 1 mM compared to ascorbic acid as positive control. Results revealed that, ZnONPs and SeONPs have strong antioxidant activity in compared to ascorbic acid, although SeONPs have antioxidant activity more than ZnONPs. Moreover, results showed EC50 (effective concentration required to inhibit 50% of free radicals) of SeONPs were 0.0078 Mm, while as EC50 of ZnONPs was 0.0312 Mm. Gunti et al. [18] evaluated the antioxidant activity for phyto-fabricated Se-NPs, and found it has excellent antioxidant activity and EC50 was 15.67 ± 1.41 µg/mL. Another study studied the efficacy of biogenic Se-NPs from an extract of ginger, where results exhibited potential antioxidant activity and EC50 was 125 µg/mL. Safawo et al. [68] synthesized ZnONPs using tuber extract of anchote (*Coccinia abyssinica* (Lam.) Cong.) and evaluated their antioxidant activity where IC_{50} was 127.24 µg/mL. Moreover, Umar et al. [69] evaluated antioxidant activity of phytosynthesized ZnONPs using *Albizia lebbeck* stem bark where IC_{50} was 48.5, 48.7, and 60.2 µg/mL for 0.1 M, 0.05 M, and 0.01 M ZnO NPs, respectively. The results strongly

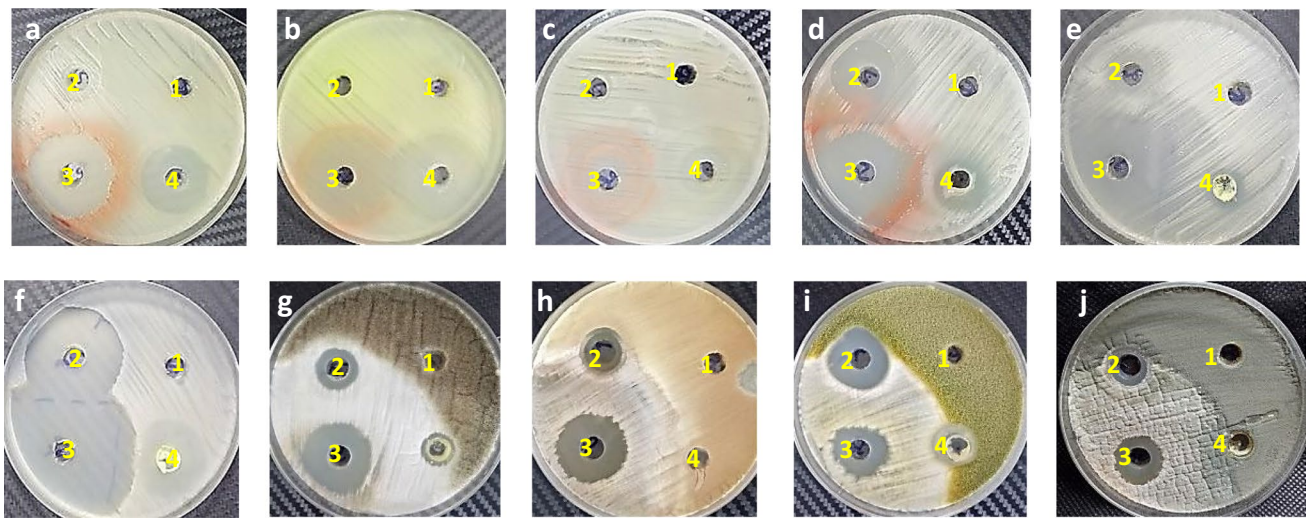

Fig. 8 Antimicrobial activity of ZnONPs and SeONPs (1 mM) against different bacterial and fungal strains (**a**–**h**): **a** *E. coli*; **b** *P. aeruginosa*; **c** *S. aureus*; **d** *B. subtilis*; **e** *C. albicans*; **f** *C. neoformans*; **g** *A. niger*; **h** *A. terreus*; **i** *A. flavus*; **j** *A. fumigatus*.1, 2, 3, and 4 mean plant extract, ZnONPs, SeONPs, and nystatin respectively

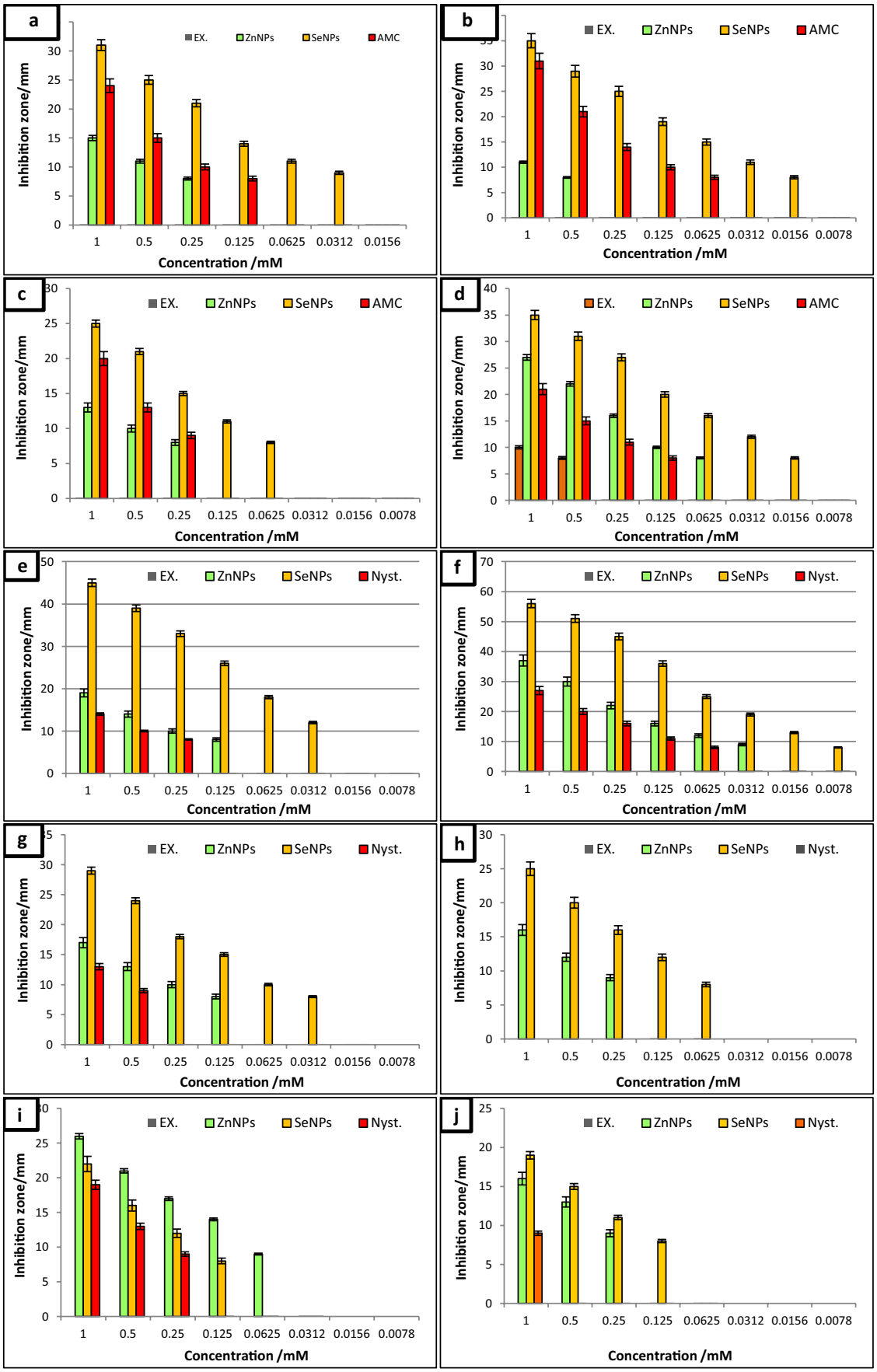
a
EX.
ZnNPs
SeNPs
AMC
Inhibition zone/mm
Concentration /mM
1
0.5
0.25
0.125
0.0625
0.0312
0.0156
b
EX.
ZnNPs
SeNPs
AMC
Inhibition zone/mm
Concentration /mM
1
0.5
0.25
0.125
0.0625
0.0312
0.0156
0.0078
c
EX.
ZnNPs
SeNPs
AMC
Inhibition zone/mm
Concentration /mM
1
0.5
0.25
0.125
0.0625
0.0312
0.0156
0.0078
d
EX.
ZnNPs
SeNPs
AMC
Inhibition zone/mm
Concentration /mM
1
0.5
0.25
0.125
0.0625
0.0312
0.0156
0.0078
e
EX.
ZnNPs
SeNPs
Nyst.
Inhibition zone/mm
Concentration /mM
1
0.5
0.25
0.125
0.0625
0.0312
0.0156
0.0078
f
EX.
ZnNPs
SeNPs
Nyst.
Inhibition zone/mm
Concentration /mM
1
0.5
0.25
0.125
0.0625
0.0312
0.0156
0.0078
g
EX.
ZnNPs
SeNPs
Nyst.
Inhibition zone/mm
Concentration /mM
1
0.5
0.25
0.125
0.0625
0.0312
0.0156
0.0078
h
EX.
ZnNPs
SeNPs
Nyst.
Inhibition zone/mm
Concentration /mM
1
0.5
0.25
0.125
0.0625
0.0312
0.0156
0.0078
i
EX.
ZnNPs
SeNPs
Nyst.
Inhibition zone/mm
Concentration /mM
1
0.5
0.25
0.125
0.0625
0.0312
0.0156
0.0078
j
EX.
ZnNPs
SeNPs
Nyst.
Inhibition zone/mm
Concentration /mM
1
0.5
0.25
0.125
0.0625
0.0312
0.0156
0.0078

◂**Fig. 9** Effect of different concentration of ZnONPs and SeONPs on bacterial and fungal strains (**a**–**h**): **a** *E*. coli; **b** *P*. aeruginosa; **c** *S*. aureus; **d** *B*. subtilis; **e** *C*. albicans; **f** *C*. neoformans; **g** *A*. niger; **h** *A*. terreus; **i** *A*. flavus; **j** *A*. fumigatus. Ex. means plant extract, AMC means amoxicillin/clavulanate, and Nyst. means nystatin

recommend the application of callus extract of *Ziziphus spina-christi*-mediated ZnONPs and SeONPs as useful natural antioxidants for health preservation against different oxidative stress associated with degenerative diseases.

3.3.9 Cytotoxicity

Biosynthesized ZnONPs and SeONPs were tested against normal human epithelial cell line: 1- BJ1 (normal Skin fibroblast) as shown in Fig. 11. The total extract appears a low cytotoxicity effect on the tested cell line where IC50 higher than 1 mM. Moreover, IC50 of both ZnONPs and SeONPs were > 0.125 and > 0.5 Mm respectively. Additionally, 0.03125 Mm of ZnONPs and SeONPs did not show any effect on the cells, and this indicates the prepared ZnONPs and SeONPs in this study are safe in use. However, the nanoparticles did not affect the shape of cells as well as not deformed the cells appears. It is well known that the toxicity of materials affects the cell performance and shape, so in our work, the produced nanoparticles may affect the atmospheric environment of cell according to their chemical behavior not toxic to the cells.

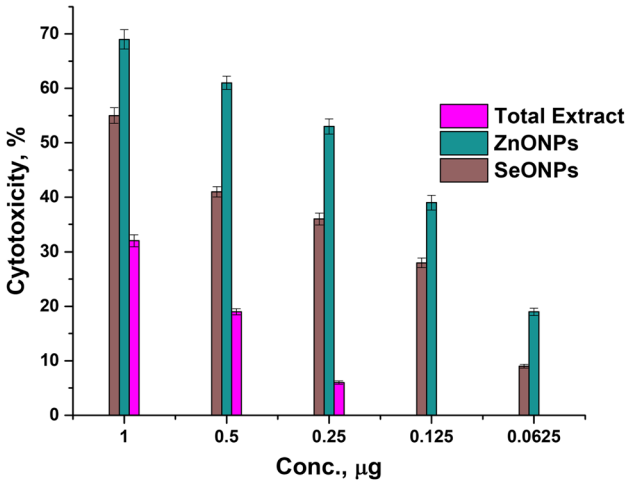

Fig. 11 The cytotoxicity test of cells at different concentrations of ZnONPs and SeONPs and total extract

4 Conclusion

In the current study, green eco-friendly biosynthesis of ZnONPs and SeONPs was performed using callus extract of *Ziziphus spina-christi* for the first time. Characterization of ZnONPs and SeONPs was performed using UV–vis, FTIR, XRD, SEM, TEM, and thermal analysis, and results revealed that different concentrations of callus extract are not affected the performance of the prepared nanoparticles as well as crystallinity. Antimicrobial activity and antioxidant activity of ZnONPs and SeONPs were evaluated, and result revealed that both of ZnONPs and SeONPs have potential

Fig. 10 Antioxidant activity of ZnONPs and SeONPs at different concentrations

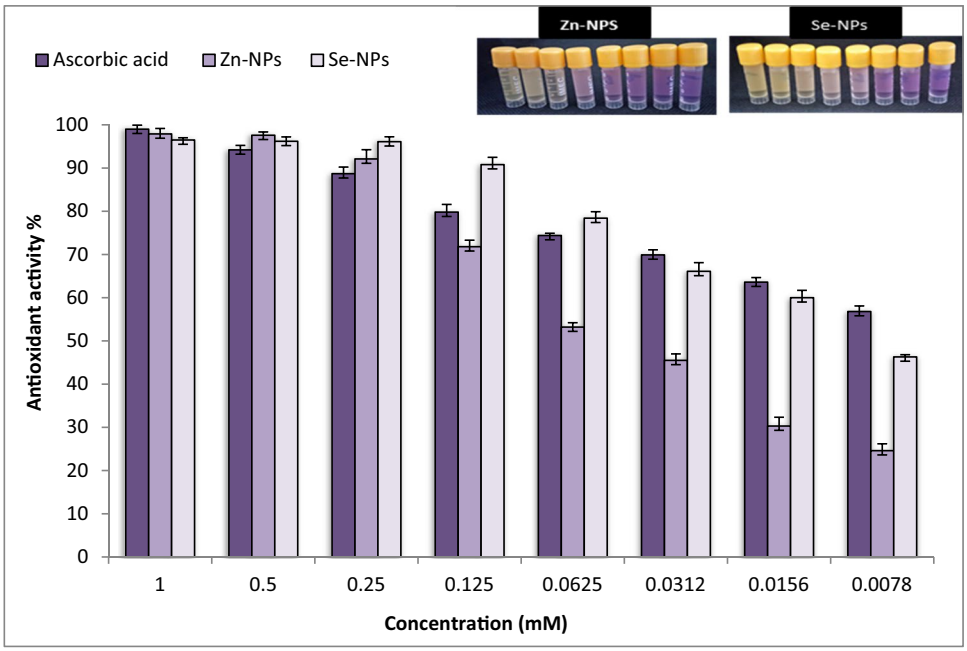

antimicrobial activity against Gram positive, negative bacteria, unicellualar, and multicellular fungi. Moreover, both of ZnONPs and SeONPs have strong antioxidant activity as well as antimicrobial activity in safe use.

Acknowledgements The authors express their sincere thanks to the Faculty of Science (Boyes), Al-Azhar University, Cairo, Egypt, for providing the necessary research facilities. The authors would like to acknowledge the facilities available at the National Research Centre of Egypt.

Declarations

Conflict of interest The authors declare no competing interests.

References

1. Sundararaj N, Kalagatur NK, Mudili V, Krishna K, Antonysamy M (2019) Isolation and identification of enterotoxigenic Staphylococcus aureus isolates from Indian food samples: evaluation of in-house developed aptamer linked sandwich ELISA (ALISA) method. J Food Sci Technol 56(2):1016–1026
2. Schmiedel Y, Zimmerli S (2016) Common invasive fungal diseases: an overview of invasive candidiasis, aspergillosis, cryptococcosis, and Pneumocystis pneumonia. Swiss Med Wkly 146:w14281
3. Dacrory S, Hashem AH, Hasanin M (2021) Synthesis of cellulose based amino acid functionalized nano-biocomplex: characterization, antifungal activity, molecular docking and hemocompatibility. Environ Nanotechnol Monit Manag 15:100453. https://doi.org/10.1016/j.enmm.2021.100453
4. Singh C, Sharma V, Naik PK, Khandelwal V, Singh H (2011) A green biogenic approach for synthesis of gold and silver nanoparticles using Zingiber officinale. Dig J Nanomater Biostructures 6(2):535–542
5. Abu-Elghait M, Hasanin M, Hashem AH, Salem SS (2021) Ecofriendly novel synthesis of tertiary composite based on cellulose and myco-synthesized selenium nanoparticles: characterization, antibiofilm and biocompatibility. Int J Biol Macromol 175:294–303. https://doi.org/10.1016/j.ijbiomac.2021.02.040
6. Hashem AH, Khalil AMA, Reyad AM, Salem SS (2021) Biomedical applications of mycosynthesized selenium nanoparticles using Penicillium expansum ATTC 36200. Biol Trace Elem Res 199(10):3998–4008
7. Ravichandran V, Vasanthi S, Shalini S, Shah SAA, Harish RJML (2016) Green synthesis of silver nanoparticles using Atrocarpus altilis leaf extract and the study of their antimicrobial and antioxidant activity. Mater Lett 180:264–267
8. Abdelraof M, Hasanin MS, Farag MM, Ahmed HY (2019) Green synthesis of bacterial cellulose/bioactive glass nanocomposites: effect of glass nanoparticles on cellulose yield, biocompatibility and antimicrobial activity. Int J Biol Macromol 138:975–985
9. Hasanin MS, Mostafa AM, Mwafy EA, Darwesh O (2018) Ecofriendly cellulose nano fibers via first reported Egyptian Humicola fuscoatra Egyptia X4: isolation and characterization. Environ Nanotechnol Monit Manag 10:409–418
10. Mostafa AM, Mwafy EA, Hasanin MS (2020) One-pot synthesis of nanostructured CdS, CuS, and SnS by pulsed laser ablation in liquid environment and their antimicrobial activity. Opt Laser Technol 121:105824
11. Abdelaziz AM, Dacrory S, Hashem AH, Attia MS, Hasanin M, Fouda HM, Kamel S, ElSaied H (2021) Protective role of zinc oxide nanoparticles based hydrogel against wilt disease of pepper plant. Biocatal Agric Biotechnol 35:102083. https://doi.org/10.1016/j.bcab.2021.102083
12. Hashem AH, Abdelaziz AM, Askar AA, Fouda HM, Khalil AMA, Abd-Elsalam KA, Khaleil MM (2021) Bacillus megaterium-mediated synthesis of selenium nanoparticles and their antifungal activity against Rhizoctonia solani in faba bean plants. J Fungi 7(3):195
13. Elbasuney S, El-Sayyad GS, Tantawy H, Hashem AH (2021) Promising antimicrobial and antibiofilm activities of reduced graphene oxide-metal oxide (RGO-NiO, RGO-AgO, and RGO-ZnO) nanocomposites. RSC Adv 11(42):25961–25975
14. Menon S, Shrudhi Devi KS, Agarwal H, Shanmugam VK (2019) Efficacy of biogenic selenium nanoparticles from an extract of ginger towards evaluation on anti-microbial and anti-oxidant activities. Colloid Interface Sci Commun 29:1–8
15. Iranifam M, Fathinia M, Rad TS, Hanifehpour Y, Khataee A, Joo S (2013) A novel selenium nanoparticles-enhanced chemiluminescence system for determination of dinitrobutylphenol. Talanta 107:263–269
16. Menon S, Rajeshkumar S, Kumar V (2017) A review on biogenic synthesis of gold nanoparticles, characterization, and its applications. Resource-Efficient Technologies 3(4):516–527
17. Elbahnasawy MA, Shehabeldine AM, Khattab AM, Amin BH, Hashem AH (2021) Green biosynthesis of silver nanoparticles using novel endophytic Rothia endophytica: characterization and anticandidal activity. J Drug Deliv Sci Technol 62:102401
18. Gunti L, Dass RS, Kalagatur NK (2019) Phytofabrication of selenium nanoparticles from Emblica officinalis fruit extract and exploring its biopotential applications: antioxidant, antimicrobial, and biocompatibility. Front Microbiol 10:931
19. Naseer M, Aslam U, Khalid B, Chen B (2020) Green route to synthesize zinc oxide nanoparticles using leaf extracts of Cassia fistula and Melia azadarach and their antibacterial potential. Sci Rep 10(1):1–10
20. Rodríguez-León E, Rodríguez-Vázquez BE, Martínez-Higuera A, Rodríguez-Beas C, Larios-Rodríguez E, Navarro RE, López-Esparza R, Iñiguez-Palomares RA (2019) Synthesis of gold nanoparticles using Mimosa tenuiflora extract, assessments of cytotoxicity, cellular uptake, and catalysis. Nanoscale Res Lett 14(1):1–16
21. Essien ER, Atasie VN, Oyebanji TO, Nwude DO (2020) Biomimetic synthesis of magnesium oxide nanoparticles using Chromolaena odorata (L.) leaf extract. Chem Pap 74:1–9
22. Chowdhury R, Khan A, Rashid MH (2020) Green synthesis of CuO nanoparticles using Lantana camara flower extract and their potential catalytic activity towards the aza-Michael reaction. RSC Adv 10(24):14374–14385
23. Luque PA, Nava O, Soto-Robles CA, Chinchillas-Chinchillas MJ, Garrafa-Galvez HE, Baez-Lopez YA, Valdez-Núñez KP, Vilchis-Nestor AR, Castro-Beltrán A (2020) Improved photocatalytic efficiency of SnO2 nanoparticles through green synthesis. Optik 206:164299. https://doi.org/10.1016/j.ijleo.2020.164299
24. Ezhilarasi AA, Vijaya JJ, Kaviyarasu K, Zhang X, Kennedy LJ (2020) Green synthesis of nickel oxide nanoparticles using Solanum trilobatum extract for cytotoxicity, antibacterial and photocatalytic studies. Surf Interfaces 20:100553. https://doi.org/10.1016/j.surfin.2020.100553
25. Masum M, Islam M, Siddiqa M, Ali KA, Zhang Y, Abdallah Y, Ibrahim E, Qiu W, Yan C, Li B (2019) Biogenic synthesis of silver nanoparticles using Phyllanthus emblica fruit extract and its inhibitory action against the pathogen Acidovorax oryzae Strain RS-2 of rice bacterial brown stripe. Front Microbiol 10:820
26. Demissie MG, Sabir FK, Edossa GD, Gonfa BA (2020) Synthesis of zinc oxide nanoparticles using leaf extract of Lippia adoensis (Koseret) and evaluation of its antibacterial activity. J Chem 2020

27. Alamdari S, Sasani Ghamsari M, Lee C, Han W, Park H-H, Tafreshi MJ, Afarideh H, Ara MHM (2020) Preparation and characterization of zinc oxide nanoparticles using leaf extract of Sambucus ebulus. Appl Sci 10(10):3620
28. Bala N, Saha S, Chakraborty M, Maiti M, Das S, Basu R, Nandy P (2015) Green synthesis of zinc oxide nanoparticles using Hibiscus subdariffa leaf extract: effect of temperature on synthesis, anti-bacterial activity and anti-diabetic activity. RSC Adv 5(7):4993–5003
29. Ogunyemi SO, Abdallah Y, Zhang M, Fouad H, Hong X, Ibrahim E, Masum MMI, Hossain A, Mo J, Li B (2019) Green synthesis of zinc oxide nanoparticles using different plant extracts and their antibacterial activity against Xanthomonas oryzae pv. oryzae. Artif Cells Nanomed Biotechnol 47(1):341–352
30. Ali K, Dwivedi S, Azam A, Saquib Q, Al-Said MS, Alkhedhairy AA, Musarrat J (2016) Aloe vera extract functionalized zinc oxide nanoparticles as nanoantibiotics against multi-drug resistant clinical bacterial isolates. J Colloid Interface Sci 472:145–156
31. Fardsadegh B, Jafarizadeh-Malmiri H (2019) Aloe vera leaf extract mediated green synthesis of selenium nanoparticles and assessment of their in vitro antimicrobial activity against spoilage fungi and pathogenic bacteria strains. Green Process Synth 8(1):399–407
32. Anu K, Devanesan S, Prasanth R, AlSalhi MS, Ajithkumar S, Singaravelu G (2020) Biogenesis of selenium nanoparticles and their anti-leukemia activity. J King Saud Univ-Sci 32(4):2520–2526
33. Alagesan V, Venugopal S (2019) Green synthesis of selenium nanoparticle using leaves extract of withania somnifera and its biological applications and photocatalytic activities. Bionanoscience 9(1):105–116
34. Mandaville JP (1990) Flora of Eastern Saudi Arabia. Kegan Paul International London
35. Said A, Huefner A, Tabl E, Fawzy G (2006) Two new cyclic amino acids from the seeds and antiviral activity of methanolic extract of the roots of Zizyphus spinachristi. Planta Medica 72(11):P_222
36. Abdel-Wahhab MA, Omara EA, Abdel-Galil MM, Hassan NS, Nada SA, Saeed A, ElSayed MM (2007) Zizyphus spina-christi extract protects against aflatoxin B1-intitiated hepatic carcinogenicity. Afr J Tradit Complement Altern Med 4(3):248
37. Classic Murashige T, Skoog F (1962) A revised medium for rapid growth and bioassays with tobacco tissue cultures. Physiologia Plantarum 15:473–497
38. Valgas C, Souza SMD, Smânia E, Smânia A (2007) Screening methods to determine antibacterial activity of natural products. Braz J Microbiol 38:369–380
39. Yildirim A, Mavi A, Kara A (2001) Determination of antioxidant and antimicrobial activities of L. extracts. J Agric Food Chem 49(8):4083–9
40. Khalil A, Abdelaziz A, Khaleil M, Hashem A (2021) Fungal endophytes from leaves of Avicennia marina growing in semiarid environment as a promising source for bioactive compounds. Lett Appl Microbiol 72(3):263–274
41. Ahmadi E, Nasr SMH, Jalilvand H (2013) Callus induction and plant regeneration from node explants of Ziziphus spina-christi. JAEB 1(1):9
42. Mamun A, Islam R, Reza M, Joadar OI (1996) In vitro differentiation of plantlet of tissue culture of Samonea saman. Plant Tissue Cult 6:1–5
43. Chee PP (1990) High frequency of somatic embryogenesis and recover of fertile cucumber plants. HortScience 25(7):792–793
44. Ahmad N, Faisal M, Anis M, Aref IM (2010) vitro callus induction and plant regeneration from leaf explants of Ruta graveolens L. S Afr Geogr J 76(3):597–600
45. Li Y, Gao J, Fei S-Z (2009) High frequency in vitro embryogenic callus induction and plant regeneration from indiangrass mature caryposis. Sci Hortic 119(3):306–309
46. Hasanin M, Al Abboud MA, Alawlaqi MM, Abdelghany TM, Hashem AH (2021) Ecofriendly synthesis of biosynthesized copper nanoparticles with starch-based nanocomposite: antimicrobial, antioxidant, and anticancer activities. Biol Trace Elem Res 1–14
47. Mittal AK, Chisti Y, Banerjee UC (2013) Synthesis of metallic nanoparticles using plant extracts. Biotechnol Adv 31(2):346–356
48. Santhoshkumar J, Kumar SV, Rajeshkumar S (2017) Synthesis of zinc oxide nanoparticles using plant leaf extract against urinary tract infection pathogen. Resource-Efficient Technol 3(4):459–465
49. Chen C, Yu B, Liu P, Liu J, Wang L (2011) Investigation of nanosized ZnO particles fabricated by various synthesis routes. Journal of Ceramic Processing Research 12(4):420–425
50. Chikkanna MM, Neelagund SE, Rajashekarappa KK (2019) Green synthesis of Zinc oxide nanoparticles (ZnO NPs) and their biological activity. SN Appl Sci 1(1):117
51. Xu C, Guo Y, Qiao L, Ma L, Cheng Y, Roman A (2018) Biogenic synthesis of novel functionalized selenium nanoparticles by Lactobacillus casei ATCC 393 and its protective effects on intestinal barrier dysfunction caused by enterotoxigenic Escherichia coli K88. Front Microbiol 9:1129
52. Dhivya A, Yadav R, Powrnika S (2019) Green synthesis of selenium doped zinc oxide nanoparticles using Mangifera indica leaf extract and its photodegradation and antibacterial activities. Journal of Nanoscience and Technology 741–744
53. Mohaddes-Kamranshahi M, Jafarizadeh-Malmiri H, Simjoo M, Jafarizad A (2019) Evaluation of the saponin green extraction from Ziziphus spina-christi leaves using hydrothermal, microwave and Bain-Marie water bath heating methods. Green Process Synth 8(1):62–67
54. Halawani E (2016) Rapid biosynthesis method and characterization of silver nanoparticles using Zizyphus spina christi leaf extract and their antibacterial efficacy in therapeutic application. J Biomater Nanobiotechnol 8(1):22–35
55. Temerk H, Salem W, Sayed W, Hassan FS (2017) Antibacterial effect of phytochemial extracts from Ziziphus-spina christi against some pathogenic bacteria. Egypt J Bot 57(3):595–604
56. Nagaraju G, Prashanth S, Shastri M, Yathish K, Anupama C, Rangappa D (2017) Electrochemical heavy metal detection, photocatalytic, photoluminescence, biodiesel production and antibacterial activities of Ag–ZnO nanomaterial. Mater Res Bull 94:54–63
57. Gunti L, Dass RS, Kalagatur NK (2019) Phytofabrication of selenium nanoparticles from Emblica officinalis fruit extract and exploring its biopotential applications: antioxidant, antimicrobial, and biocompatibility. Front Microbiol 10:931
58. Kannan S, Mohanraj K, Prabhu K, Barathan S, Sivakumar G (2014) Synthesis of selenium nanorods with assistance of biomolecule. Bull Mater Sci 37(7):1631–1635
59. Sangeetha G, Rajeshwari S, Venckatesh R (2011) Green synthesis of zinc oxide nanoparticles by aloe barbadensis miller leaf extract: structure and optical properties. Mater Res Bull 46(12):2560–2566. https://doi.org/10.1016/j.materresbull.2011.07.046
60. Kargarzadeh H, Ahmad I, Abdullah I, Dufresne A, Zainudin SY, Sheltami RM (2012) Effects of hydrolysis conditions on the morphology, crystallinity, and thermal stability of cellulose nanocrystals extracted from kenaf bast fibers. Cellulose 19(3):855–866
61. Abdelraof M, Hasanin MS, El-Saied H (2019) Ecofriendly green conversion of potato peel wastes to high productivity bacterial cellulose. Carbohydr Polym 211:75–83
62. Kumar A, Dixit CK (2017) 3 - Methods for characterization of nanoparticles. In: Nimesh S, Chandra R, Gupta N (eds) Advances in nanomedicine for the delivery of therapeutic nucleic acids. Woodhead Publishing 43–58. https://doi.org/10.1016/B978-0-08-100557-6.00003-1

63. Shoeibi S, Mashreghi M (2017) Biosynthesis of selenium nanoparticles using Enterococcus faecalis and evaluation of their antibacterial activities. J Trace Elem Med Biol 39:135–139. https://doi.org/10.1016/j.jtemb.2016.09.003
64. Kokila K, Elavarasan N, Sujatha V (2017) Diospyros montana leaf extract-mediated synthesis of selenium nanoparticles and their biological applications. New J Chem 41(15):7481–7490
65. Zonaro E, Lampis S, Turner RJ, Qazi SJS, Vallini G (2015) Biogenic selenium and tellurium nanoparticles synthesized by environmental microbial isolates efficaciously inhibit bacterial planktonic cultures and biofilms. Front Microbiol 6:584
66. Yamamoto O (2001) Influence of particle size on the antibacterial activity of zinc oxide. Int J Inorg Mater 3(7):643–646. https://doi.org/10.1016/S1466-6049(01)00197-0
67. Cui J-L, Guo T-T, Ren Z-X, Zhang N-S, Wang M-L (2015) Diversity and antioxidant activity of culturable endophytic fungi from alpine plants of Rhodiola crenulata, R. angusta, and R. sachalinensis. PloS one 10(3):e0118204
68. Safawo T, Sandeep BV, Pola S, Tadesse A (2018) Synthesis and characterization of zinc oxide nanoparticles using tuber extract of anchote (Coccinia abyssinica (Lam.) Cong.) for antimicrobial and antioxidant activity assessment. OpenNano 3:56–63. https://doi.org/10.1016/j.onano.2018.08.001
69. Umar H, Kavaz D, Rizaner N (2018) Biosynthesis of zinc oxide nanoparticles using Albizia lebbeck stem bark, and evaluation of its antimicrobial, antioxidant, and cytotoxic activities on human breast cancer cell lines. Int J Nanomed 14:87–100. https://doi.org/10.2147/IJN.S186888